IV International Conference on Computational Methods for Coupled Problems in Science and Engineering
COUPLED PROBLEMS 2011
M. Papadrakakis, E. Oñate and B. Schrefler (Eds)

EXPERIMENTAL BENCHMARK AND NUMERICAL VALIDATION OF A FREE HEAVING AIRFOIL

J.J.H.M. STERENBORG*, A.H. VAN ZUIJLEN* AND H.BIJL*

*Delft University of Technology, faculty of Aerospace Engineering,
Kluyverweg 1 2629 HS Delft,
The Netherlands
e-mail: j.j.h.m.sterenborg@tudelft.nl

Key words: Heave, fluid-structure interaction, experimental benchmark, URANS, panel code, theodorsen

Abstract. In order to validate fluid-structure interaction solvers, a one degree of freedom (1 DOF) aeroelastic experiment is performed. A rigid wing with an harmonically actuated flap, is suspended by springs to allow a free heaving motion. Displacements and time dependent aerodynamic forces are measured for reduced flap frequencies ranging from $k = 0.1$ to $k = 0.3$. Simulations with three codes of different complexity level are performed for validation purposes: theodorsens model, a 2D panel code and 2D URANS, all coupled to a 1 DOF structural model. Results presented by bode diagrams, show differences in both the displacement and the lift between numerical work and experiment. Although there is an offset, consistency is found between displacements, forces and phase angles in the system for all simulations and the experiment.

1 INTRODUCTION

In many applications the interaction between fluid and structures is important to consider. Examples are deformations of aircraft, buildings, bridges and wind turbines due to airloads. Fluid-structure interactions (FSI) can be investigated in several ways. It is very common to use a numerical approach for solving a particular case [1, 2, 6]. However, the problem with many numerical FSI solvers is that the validation with measurement data is relatively unexplored. Some validations are performed, but as far as noticed they all have there restrictions, e.g. very low Reynolds numbers [7] or prescribed motions [3]. In general one can say that without a decent validation it means that it is not proven that the equations that are solved, tackle the problem in the correct way.

Another option is to perform field measurements: existing structures equipped with sensors gather the necessary data. Field measurements are e.g. performed on wind turbines. However, the problem with such methods is that it is almost impossible to

know the exact boundary conditions. This implies the data can often only be used for a qualitative assessement. Validation of numerical solvers is not likely to be possible with these datasets.

A third option is to perform experiments in a wind tunnel with a (scale) model. This provides direct insight in fluid-structure interactions, although also in wind tunnel measurements one has to deal with uncertainties and measurement errors. Benifit is that when uncertainties and measurement errors are considered and quantified, the measurement data can be used for validation purposes.

This research is performed to be able to validate FSI solvers for Reynolds numbers in the order of one million. The focus is on a controlled experiment in the wind tunnel involving FSI. The complexity level is reduced as much as possible and has led to a one degree of freedom aeroelastic experiment: a free heaving airfoil with an actuated 20% chord trailing edge flap. Forces and displacements are measured by sensors.

Next to the experiment, for validation an URANS solver, a 2D panel code and Theordorsens model, all coupled to a structural model, are used to simulate the same test case. The solutions are compared with the experimental results.

2 EXPERIMENT AND METHODS

For both the experiment and the numerical modeling it is benificial to keep the complexity level as moderate as possible. Therefore, a rigid body is considered with only one degree of freedom: the vertical or heaving motion. Since the structure is rigid the structural model can be modeled by a mass-damper-spring system, as shown in Figure 1.

The wing (mass m) is excited by a time dependent lift force F. The lift force is fluctuating due to a prescribed, harmonic actuated flap motion and the wing motion. By applying different flap frequencies the response of the system and thus the fluid-structure interactions can be assessed. Since the wing is mounted in between side panels, another simplification is made: the flow can be approximated to be two dimensional for angles of attack in the linear part of the $c_l - \alpha$ curve. This assumption is checked by observing the spanwise flow component with tufts covering about 75% of the span width, although some losses of lift near the edges are unavoidable.

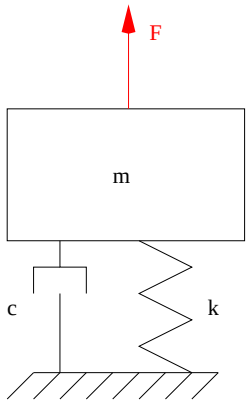

Figure 1: 1 DOF structural model

2.1 EXPERIMENTAL SETUP

The experiment is conducted in the Open Jet Facility (OJF) of Delft University of Technology.

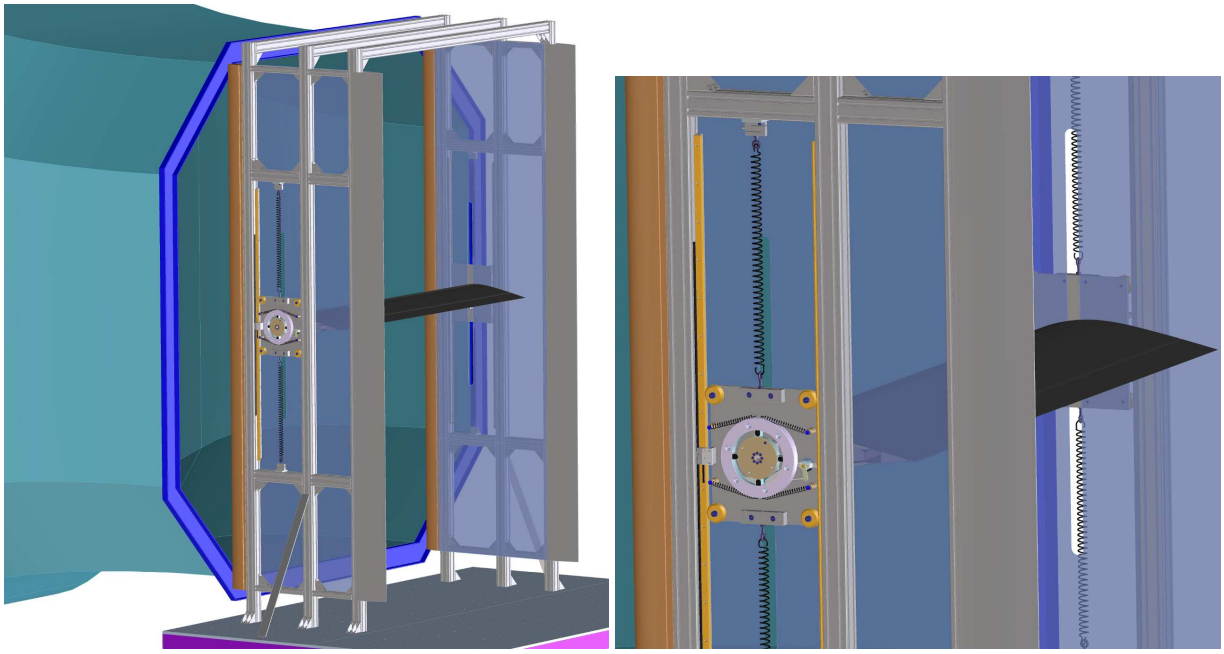

(a) Experimental setup (b) Detail of suspension

Figure 2: Experimental setup: (a) overview and (b) detail of suspension

The wind tunnel is characterized by an open test section of 2.85m x 2.85m. The typical turbulence level in this tunnel at the measurement wind speed of 21m/s is below 0.5%. At the test section an adjustable flat table is present to mount a test model. The plateau is positioned about 20 cm below the exit, such that the jet can expand also downwards.

On the plateau a supporting frame with a height of 3.2m, a width of 2m and a length of 1.03m is mounted. This frame accommodates sensors, a rails system, spring systems and two side plates that can translate along the rails. In Figure 2(a) an schematic overview is given of the experimental setup.

The wing is attached with bearings to two side plates that can slide along rails in vertical direction, as can be seen in 2(b). The side plates are suspended to the frame by 4 sets of springs, that are pre-tensioned. The amount of pre-tension is not important as long as it is such that the springs for each possible position of the wing are loaded. The springs have a joint theoretical stiffness of $k_s = 8550.3$N/m. The mechanism for the pitching motion, as can be seen in the same figure is locked. The carbon-fibre wing is an extrusion of a DU96-W180 airfoil with a full span 20% chord trailing edge flap. The flap is hinged at the lower surface and actuated by two servo engines installed in the wing. Turbulator strips are applied at the suction surface at 2% of the chord from the leading edge and on the pressure side at 5% of the chord. The wing has a chord of 0.5m, yielding a Reynolds number of Re = 700000 and the span is 1.8m. The natural frequency of the entire setup is estimated to be 2.58Hz.

Various measurement devices are used in the setup, which are read out with a rate of 2000Hz. An inductive potentiometer in the wing measures the flap angle with an accuracy of $\pm 0.1^\circ$. The angle of attack is kept constant and is measured with an inclinometer with the same accuracy: $\pm 0.1^\circ$. The vertical displacement is measured by a linear encoder with an accuracy of 0.1mm. Forces are measured in two ways: two full wheatstone bridges (strain gauges) on each wing axis measure forces perpendicular and parallel to the wing chord, loadcells on each spring set (4x) measure the vertical force in the springs, with an accuracy of ± 0.2N. All signals are filtered using a low-pass Butterworth filter with a corner frequency 8Hz above the highest dominating frequency.

2.2 FREQUENCY RESPONSE AND FLAP ACTUATION

For dynamic systems the frequency response can be assessed by applying input signals with different frequencies. For the system under consideration, this means the harmonic flap actuation frequency must be changed. The harmonic motion is characterized by the reduced frequency, according to equation (1):

$$k = \frac{\pi f c}{V}, \tag{1}$$

where f is the flap frequency, c is the chord and V the freestream velocity. The reduced frequency is ranging from $k = 0.1$ up to $k = 0.3$, with steps of $\Delta k = 0.025$. This range is chosen to be around the natural frequency of the system, which is about $k = 0.2$ and with large enough tails to capture the frequency response to a large extent. Hereby, the limitations are given by the servo engines. The flap amplitude is set to $\delta_{flap} = \pm 2^\circ$. The angle of attack is chosen to be $\alpha = 0$, in order to assure attached flow. This implies that when the flap is actuated in a harmonic manner, the responses are harmonic as well.

The frequency response is found by looking at the gain M and the phase angle Ψ between combinations of input and output signals. In the frequency domain, for a standard mass-damper-spring system, the transfer function $G(s)$, gain M and phase angle Ψ can be written as:

$$G(s) = \frac{1}{(s + \zeta\omega_n + j\omega_d)(s + \zeta\omega_n - j\omega_d)}, \tag{2}$$

$$M = |G(s)|, \tag{3}$$

$$\Psi = \angle G(s) = \arctan\left(\frac{Im[G(s)]}{Re[G(s)]}\right), \tag{4}$$

with the natural frequency ω_n, the damping ratio ζ and the damped natural frequency

ω_d given by:

$$\begin{aligned} \omega_n &= \sqrt{\frac{k_s}{m}}, \\ \zeta &= \frac{c}{2\sqrt{k_s m}}, \\ \omega_d &= \omega_n \sqrt{1-\zeta^2}. \end{aligned} \tag{5}$$

In the equations m is the total mass, k_s is the combined spring stiffness and $j = \sqrt{-1}$. The mass-damper-spring system relation (2) is valid in case the lift force is used as input and the displacement is the output, meaning the experimental results can be checked accordingly. However, the lift is determined as a function of the displacement and thus the transfer function (2) is used in the reversed manner. Result is that the found phase lag between lift and displacement is in fact a lead.

2.3 FORCE DERIVATION

The forces measured by the strain gauges (SG) and the load cells (LC) are not the lift and drag forces. Consider the wing on which the lift force L, an added mass force, the drag force D, a vertical inertial force and the strain gauges forces in normal F_n and tangential direction F_t are acting on the left and the right axis. For the horizontal (x-direction) and vertical (y-direction) force equilibrium the following set of equations can be derived:

$$D = (F_{t,left} + F_{t,right}) \cos\alpha + (F_{n,left} + F_{n,right}) \sin\alpha, \tag{6}$$

$$L = (m_{wing} + m_a)\, \ddot{y} + (F_{n,left} + F_{n,right}) \cos\alpha - (F_{t,left} + F_{t,right}) \sin\alpha. \tag{7}$$

In formula (7) the mass of the wing is given by m_{wing} and the added mass is given by m_a. The added mass force is determined by considering the difference in force responses to a initial exitation of the wing and the force response to a similar initial exitation, but than with a equivalent mass (slender bar) instead of the wing. The added mass is found to be 2.31kg. Using the forces measured by the load cells F_{lc}, equations can be derived for the lift force, making use of the structural model as shown in Figure 1.

$$L = (m_s + m_a)\, \ddot{y} + (c_a + c_s)\, \dot{y} + F_{lc}, \tag{8}$$

In this equation the damping coefficients c_a and c_s appear. The aerodynamic damping coefficient c_a is found by applying an initial displacement to the wing in tunnel on conditions and measure the decay of the displacement. For the structural damping c_s the wing must be replaced by a bar with equivalent weight and the same procedure can be followed as for obtaining the aerodynamic damping. The total damping coefficient c per test case can also be found by equating relations (7) and (8). The spring stiffness k_s can be checked by measuring the vertical forces and the offset of the wing in vertical direction

from the mid of the structure in tunnel off conditions. For the combined damping coefficient c_{tot} a typical value of about 100Ns/m is observed and for the structural stiffness $k_s = 8225.3$N/m is measured. The stiffness k_s is 325N/m less compared to the theoretical value.

3 NUMERICAL WORK

Three simulations are performed with solvers of different complexity level: Theodorsens model, a panel code and an unsteady Reynolds averaged Navier-Stokes (URANS) flow solver, all coupled to a structural model. The simplest model is Theodorsens model, marching in time with a explicit 4th-order Runge-Kutta scheme. It is loosely coupled to the 1 DOF structural model, without the possibility for subiterations.

A more complex aerodynamic model is a free wake 2D panel code. To an existing code a structural model is coupled with an explicit Euler time stepping scheme and the same loose coupling as for Theodorsens model. A routine is implemented to move the flap panels according to the prescribed actuation. The flap motion is performed each time step, before the FSI displacement is computed. The total displacement for each panel is simply the sum of both contributions, since the body is rigid.

The model with the highest complexity level is an URANS flow solver coupled to a generic structure solver. The flow solver handles unstructured, hexahedral meshes and turbulence is taken care of by the Spalart-Allmaras (SA) turbulence model. The SA turbulence model is chosen because it is able to adequately solve attached flow cases. The FSI solver is loosely coupled and allows for subiterations. The flap motion is implemented in the source code in the same manner as for the 2D panel code.

As mentioned for dynamic systems it is important to predict/know the frequency response of the system. Therefore, for all three different codes a similar like interval of reduced frequencies as for the experiment is covered. Time and spatial convergence studies are performed as well, but not treated in this paper.

4 RESULTS

The setup of the experiment allows to concentrate on the force equilibrium and the displacements in the vertical direction. Since the responses are found to behave harmonically according to the input of the flap, all variables are represented as a function of the flap phase angle. The flap phase angle ϕ is given by:

$$\phi = 360(ft - k), \qquad k = 0, 1, 2, ... \quad \text{and} \quad 0^\circ \leqq \phi \leqq 360^\circ. \tag{9}$$

In this relation t is the time and f the flap frequency. The harmonic behaviour of all responses has another advantage: all signals can be phase-averaged over a large number of samples to average out small fluctuations. This is done for both the experimental results as well as for the numerical work.

For a reduced frequency range of $k = 0.1$ to $k = 0.3$ the focus is on the lift force and the vertical displacement, both as a function of ϕ, and the phase lag between the signals.

Also the phase lag of the signal with respect to the flap deflection is considered. Use is made of the bode plot to summarized the frequency responses of the system variables for the ease of comparison.

4.1 EXPERIMENTAL RESULTS

For each reduced frequency a measurement is performed of about 5 minutes. From this data set, phase averaged signals can be constructed for one full period ($\phi = 0^\circ$ to $\phi = 360^\circ$). In Figure 3 an example is given of a phase averaged result for the lift coefficient for $k = 0.2$ with the phase angle ϕ. Lift coefficients are computed making use of equation (7) and (8). In the same figure also the spread of the data is given by making use of boxplots indicating the the mean and the spread of the data.

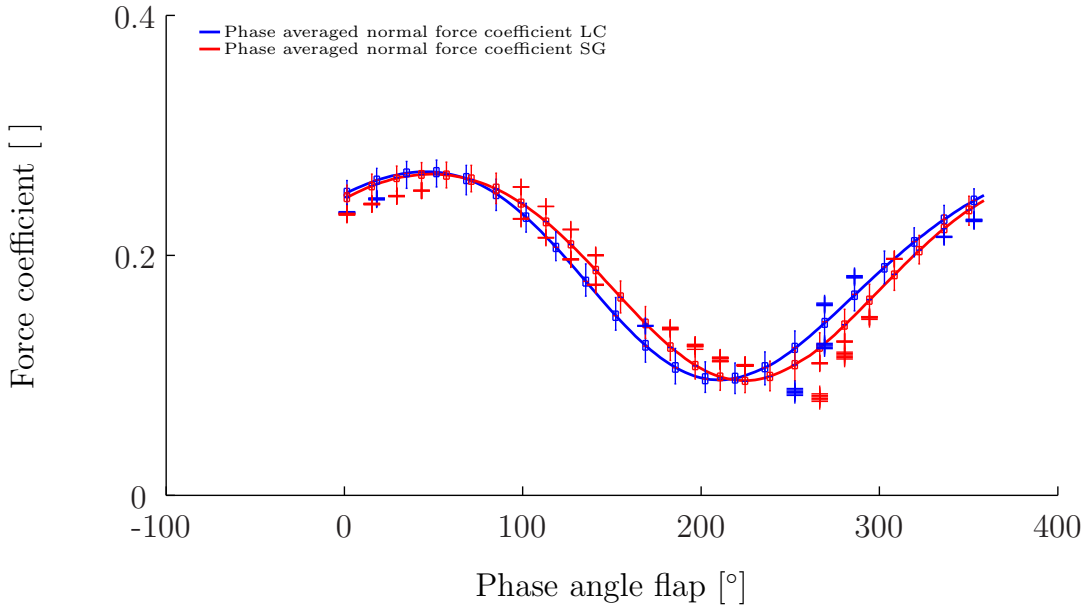

Figure 3: Phase-averaged lift coefficient, $k = 0.2$, $v = 21m/s$, $\delta_{flap} = \pm 2^\circ$

From the figure some important conclusions can be drawn. The deviations of the lift coefficients are acceptable, since 50% of the data is within 4% of the mean lift coefficient and 75% of the data is within about 10% of the mean value. Furthermore, it is noticed there is a small difference in the phase between the lift coefficient based on the strain gauges and the load cells of about maximum 8°, with the load cells leading. Most concerning however, is the mean value of the lift which is about $c_{l,mean} = 0.1878$. This is far from the static lift coefficient $c_{l,\alpha=0} = 0.285$ found in previous measurements. Possible cause might be an offset in the angle of attack or an wind tunnel related change in effective angle of attack.

To get a better understanding of the interaction between the flow and the structure, and than in particular the phase lags, the phase-averaged lift and displacement with the flap phase angle ϕ are plotted together for $k = 0.2$ in Figure 4.

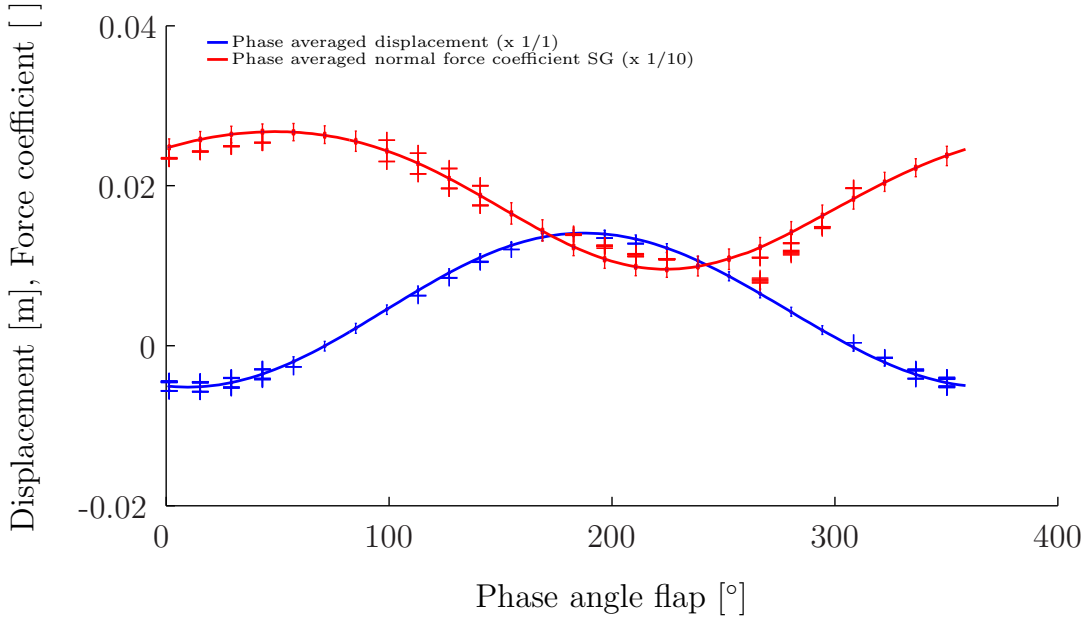

Figure 4: Phase-averaged lift coefficient, $k = 0.2$, $v = 21m/s$, $\delta_{flap} = \pm 2°$

The displacement y is plotted with respect to the initial position (wind off). It can be seen that the displacement is oscillating around a mean value of about $y = 0.0047$m with an amplitude of 0.0096m. It can be seen that the lift generation and the vertical displacement of the wing are out of phase with a lag in the lift of about 148°. Observing the same figure, the delays of the aerodynamic force and kinematic response of the wing with respect to the flap deflection is found. Apparently, the maximum lift for a reduced frequency of $k = 0.2$ is reached before the flap is fully deflected downwards. In previous research [5], it was found that in the case of an oscillating flap (no moving wing) the maximum lift occurs at maximum downward flap deflection. This implies that the motion of the wing and the resulting change in the effective angle of attack, causes the shift of the maximum lift with the flap deflection with respect to non-moving wing case.

As mentioned all previous demonstrated results can be combined in a bode diagram for all measurements. In Figure 5 the gain and the phase delay are presented for $k = 0.1$ to $k = 0.3$. Also the exact solution is plotted for the transfer function (2).

The bode diagram shows that for frequency ratios $\ll 1$ the phase delays are small and increase with increasing frequency ratio up to about $\phi = 180°$. Furthermore it can be seen that the trends are according to the exact solution for a mass-damper-spring system.

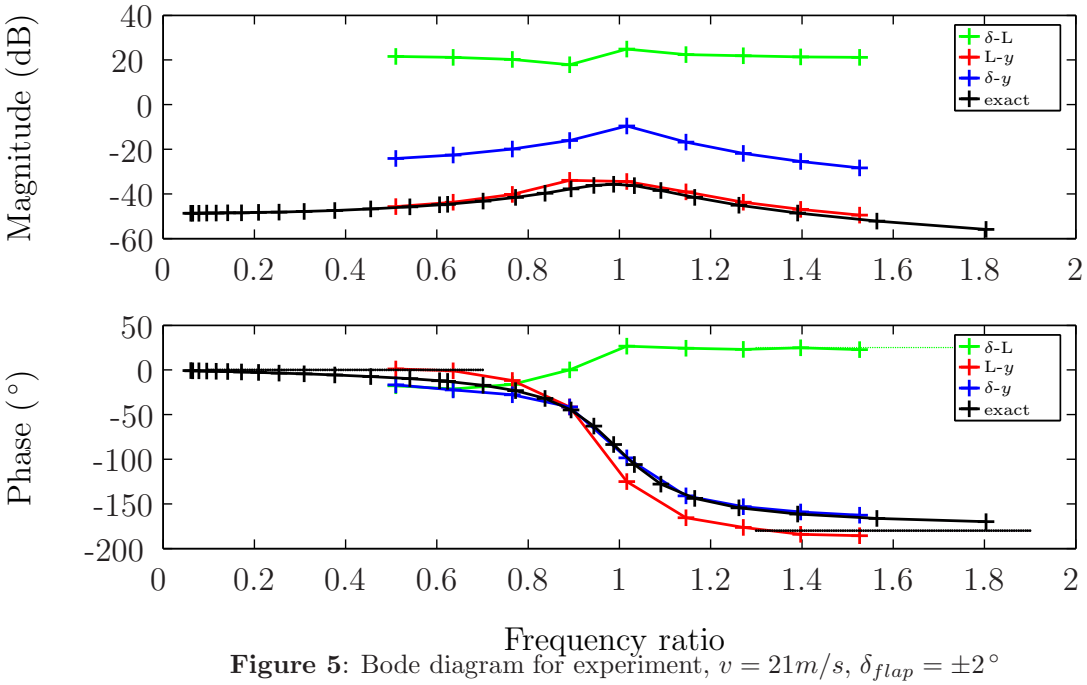

Figure 5: Bode diagram for experiment, $v = 21m/s$, $\delta_{flap} = \pm 2°$

4.2 NUMERICAL RESULTS

The numerical results are presented for Theodorsens model, the 2D panel code and the URANS model separately. For all simulations the free stream velocity is $v = 21$m/s and the flap is deflected for each reduced frequency in a similar fashion as in the experiment: $\delta_{flap} = \pm 2°$. The computations are performed for the same reduced frequencies: $k = 0.1$ to $k = 0.3$. For Theodorsens model and the panel code the structural parameters are scaled for a 2D approach: $m = 16.75$kg, $c_{tot} = 56.64$Ns/m and $k_s = 4922.45$N/m, whereas the 2D URANS simulation do not need scaling.

Theodorsens model is written according to previous work [4]. It is a 2D approximation without any modeling of wind tunnel or supporting structure interferences. The used time step is $\Delta t = 0.005$s. In Figure 6 the bode diagram is given for the simulations performed with the coupled Theodorsens model, along with the exact solution.
It follows from the bode diagram that both the magnitude and the phase show a similar tendency as the experimental results and the exact solution. However, only the magnitude of the flap-displacement curve is at nearly the same level as for the experiment. The other curves show quite an offset with respect to the experimental data, which means the predicted lift, as expected, is different compared to the experiment: for $k = 0.2$ $c_{l,mean} = 0.27$ whereas the experimental value is about $c_{l,mean} = 0.185$. As a consequence the displacements is shifted with $\Delta y = 0.0027$m such that $y_{mean} = 0.0074$m. The phase angles are of the same order as the exact solution.
Just like Theodorsens model, the 2D panel code does also not correct for aerodynamic

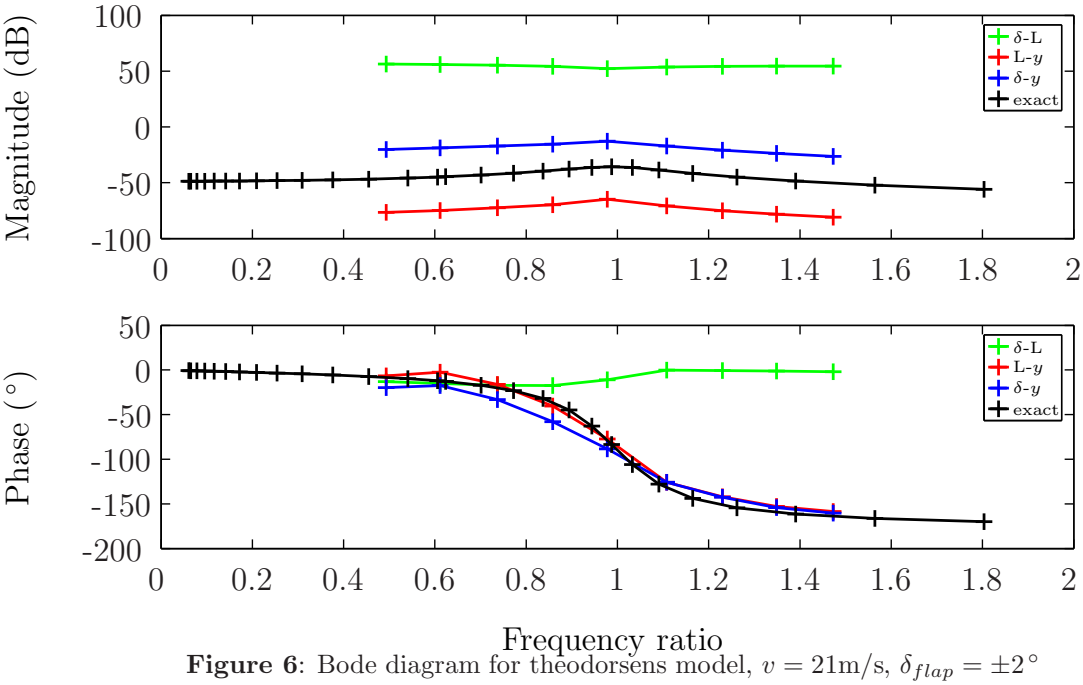

Figure 6: Bode diagram for theodorsens model, $v = 21\text{m/s}$, $\delta_{flap} = \pm 2°$

interference. The airfoil is reconstructed with 200 panels and the free wake contains maximum 1500 vortex elements. The time step is similar as used in Theodorsens model: $\Delta t = 0.005$. Figure 7 shows the bode diagram for the 2D panel code coupled to the 1 DOF structural model.

The gain of the various inputs is very similar to the gains found with Theodorsens model. For the phase angles it is seen that the trends are similar as for the experiment, except for the L-y phase lag for frequency ratios > 1. For $k = 0.2$ the mean lift coefficient is $c_{l,mean} = 0.255$ and the mean displacement is $y_{mean} = 0.0114\text{m}$. The predicted lift is of the same order as found with Theodorsen, the displacement is not corresponding the change in lift.

The URANS flow solver, with the turbulence modeled by the Spalart-Allmaras equation, is marching in time with $\Delta t = 0.005$. The free stream turbulence level is set to be of the same order as for the experiment. Computations are performed with an unstructured hexahedral mesh containing 70k cells. The bode plot is found in Figure 8.
It can be clearly seen that the results found with the URANS solver and Theodorsens model are very similar. The mean lift coefficient, which is about $c_{l,mean} = 0.299$, is the most off from the experimental lift coefficient, but comparable to the static value of $c_{l,\alpha=0} = 0.285$. The mean displacement is scaled according to the lift coefficient to a value of $y_{mean} = 0.0081\text{m}$. For the phase angles a very close approximation is found with respect to the exact solution, just like the solution found with Theodorsens model.

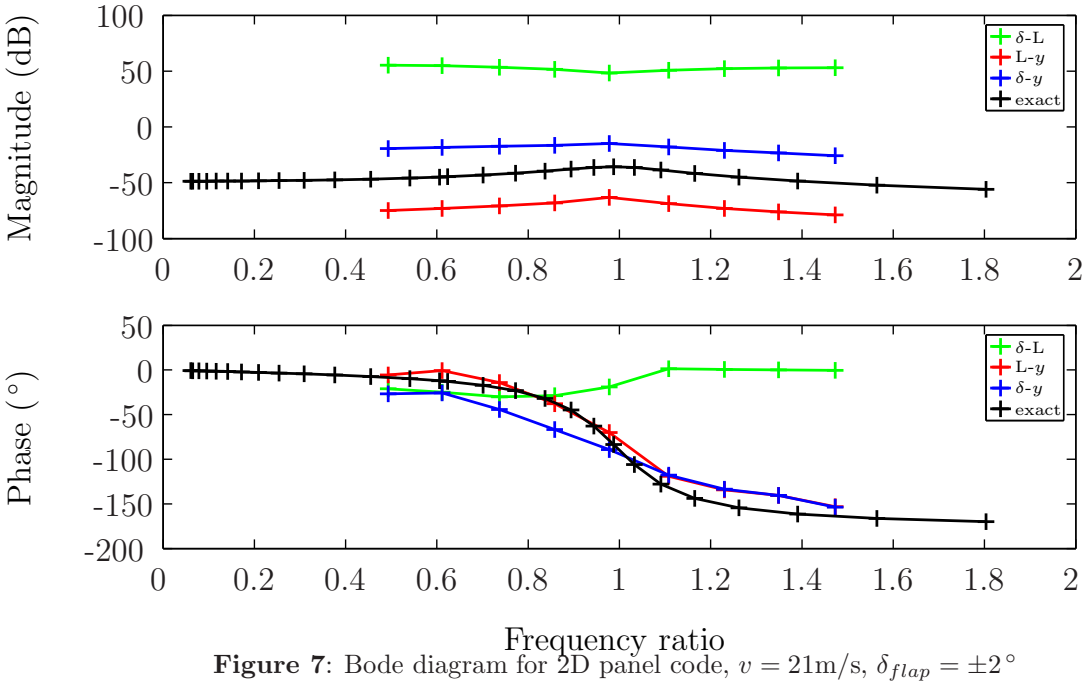

Figure 7: Bode diagram for 2D panel code, $v = 21\text{m/s}$, $\delta_{flap} = \pm 2^\circ$

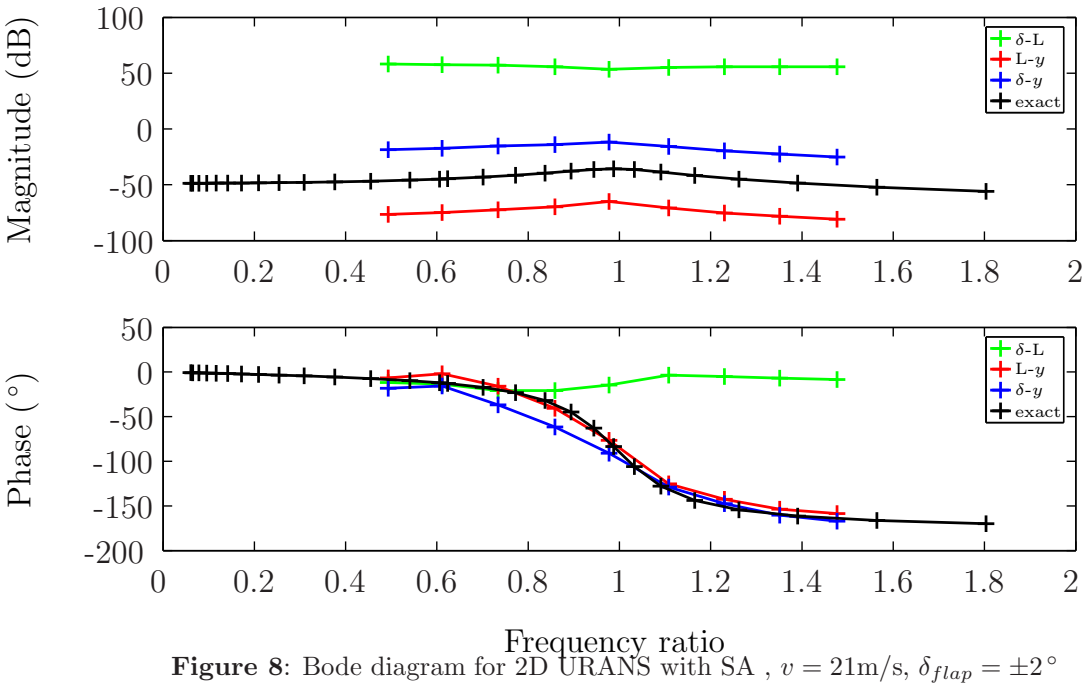

Figure 8: Bode diagram for 2D URANS with SA , $v = 21\text{m/s}$, $\delta_{flap} = \pm 2^\circ$

5 CONCLUSIONS

A 1 DOF aeroelastic experiment is performed: a freely heaving rigid wing with a 20%c trailing edge flap. The flap is actuated harmonically with an amplitude of $\delta_{flap} = \pm 2^\circ$

over an reduced frequency range of $k = 0.1$ to $k = 0.3$. Amongst others the aerodynamic lift, the wing displacement and the flap angle are measured. For validation simulations are performed with Theodorsens model, a 2D panel code and a 2D URANS solver with SA turbulence modeling, all coupled to a 1 DOF structural model.

The experiment shows good agreement with the exact solution for a standard mass-damper-spring system. Concerning is the offset of the found mean lift coefficient with respect to the static lift coefficient for the same constant angle of attack: $c_{l,mean} = 0.1878$ and $c_{l,\alpha=0} = 0.285$ respectively. The good coherence of the experimental results with the exact solution indicate there might be an offset in the angle of attack, but further research is needed. The phase angles are according the expectancy: almost no lag for frequencies much smaller than the eigenfrequency and for frequency above the eigenfrequency asymptotic behaviour is found towards $\phi = 180°$.

The numerical solutions confirm that the experiment is off, since the mean lift values are all close to the mean static lift value. The found displacements are consist with the offset in the lift, except for a slightly higher prediction of the displacment for the panel code. The phase angles are close to expectancy.

References

[1] A.D. Gardner et al. Simulation of Oscillating Airfoils and Moving Flaps Employing the DLR-TAU Unsteady Grid Adaptation. In *New Results in Numerical Fluid and Experimental Fluid Mechanics VI*, volume Vol. 96/2008 of *Notes on Numerical Fluid Mechanics and Multidisciplinary Design*, pages 170–177. Springer Berlin/Heidelberg, 2008.

[2] Joseph A. Garcia. Numerical investigation of nonlinear aeroelastic effects on flexible high aspect ratio wings. *Journal of aircraft*, 2005.

[3] P. Gerontakos and T. Lee. Piv study of flow around unsteady airfoil with dynamic trailing-edge flap deflection. *Experiments in Fluids*, 45:955–972, 2008.

[4] J. Gordon Leishman. Unsteady lift of a flapped airfoil by indicial concepts. *Journal of aircraft*, 31.

[5] R.C.J. Lindeboom, J.J.H.M. Sterenborg, and C.Simao. Determination of unsteady loads on a du96w180 airfoil with actuated flap using particle image velocimetry. In *The Science of making Torque from Wind*, 2010.

[6] V. Riziotis, A. Hizanidi, and S.G. Voutsinas. Aeroelastic stability analysis of wind turbine blades using CFD techniques. *NTUA publication*.

[7] J.M.A. Stijnen, J. de Hart, P.H.M. Bovendeerd, and F.N. van de Vosse. Evaluation of a fictitious domain method for predicting dynamic response of mechanical heart valves. *Journal of fluids and structures*, 19, 2004.